Realization, characterization and measurements of standard leak artefacts

Realization, characterisation and measurements of standard leak artefacts

Ute Becker[5], Djilali Bentouati[3], Mercede Bergoglio[2], Frédéric Boineau[3],
Wolfgang Jitschin[4], Karl Jousten[5], Domenico Mari[2], Dominik Prazak[1], Martin Vicar[1]

[1] *Cesky Metrologicky Institut (CMI), Czech Republic*
[2] *Istituto Nazionale di Ricerca Metrologica (INRIM), Italy*
[3] *Laboratoire National de mètrologie et d'Essais (LNE), France*
[4] *Technische Hochschule Mittelhessen (THM), Germany*
[5] *Physikalisch Technische Bundesanstalt (PTB), Germany*

Email of corresponding author: d.mari@inrim.it

Abstract

Predictability of gas flows through leak elements in various conditions (geometry of leak elements, gas species, pressure) from the results of only a few measurements in a specific configuration is an issue for the gas dynamics theory. This paper aims to provide results of leak flow rate measurements performed by national metrology institutes (NMIs) in the framework of the European project JRP IND12. Leak artefacts made of different materials with well defined geometry, were calibrated by means of primary standards with different gas species flowing to vacuum or atmospheric pressure. The numerous collected data are made available to allow the experts in gas dynamics to use this large database to improve the knowledge of gas flow in narrow ducts in terms of predictability for different gas species and find a simple model to describe the gas flow inside microchannels.

Keywords: gas flow metrology, standard leak artefacts, experimental data set

1. Introduction

Development of the theory of gas flow in narrow ducts is an objective related to improvement of leak measurement and testing. At present, the leaks generally used in the industrial environment are obtained by crimping small stainless steel capillaries [1, 2, 3], which usually work in the 10^{-5} mbar L/s – 10^{-3} mbar L/s range suitable for leak testing. Due to the unknown geometry and flow characteristic, even an empirical description of gas flow rate is difficult to achieve. Therefore it was decided to realize leak elements with well-defined geometry. The artefacts have been characterized geometrically and the flow rate measured with primary standards [4-9] against vacuum and atmospheric pressure for

different gases. In the first part of the paper, the description of the realization and geometrical characterization is reported. In the second part a short description of the primary systems used for the characterization is presented and the third part is related to the measurement results. This data collection will be useful to the fluid dynamics experts to find a simple model to describe the regime inside the ducts from molecular to hydrodynamic and suggest to the leak testing operator how to predict the gas flow in other conditions (in particular, different gases), starting from a small sample of measurements performed with only one species of gas.

2. Leak artifacts realization

Different kinds of leak elements were realized to provide new types of leak artefacts. The leaks were designed with the purpose of supplying a product suitable for industrial applications.

2.1. Glass capillary

Five glass capillaries were supplied by Danfoss company (Denmark) having nominal gas flow rate values between $1x10^{-6}$ mbar L/s and $1x10^{-5}$ mbar L/s at 1 bar with reference to vacuum. The scheme of capillary geometry is shown in Fig. 1a.

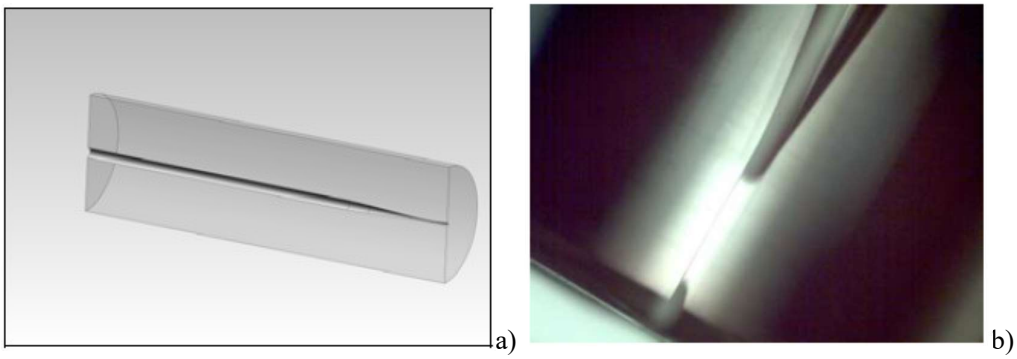

Fig. 1 a) Schematic of a glass capillary; b) restriction of the duct

The restriction inside the glass tube has been obtained with the following procedure: the glass capillary is connected to the leak detector unit and, in principle, the leak element is used as a "sniffer" leak detecting device. The glass is then heated uniformly by using a special burner device (two heads). As the glass is heated at a specific point (burner on and off to prevent closure of the element), the capillary slowly contracts, forming a restriction (leak element). During this procedure helium is blown on top of the glass leak element and leak rate is measured with the leak detector (pressure difference of 1 bar). Leak elements generating gas flow greater than $5x10^{-7}$ mbar L/s can be produced. After cooling, the element is cut to have the final length (>1 cm) by using a glass cut device. The glass leaks

were observed using an optical microscope: in Fig. 1b the restriction of the duct has been made visible.

Two of the supplied capillaries were used for the measurements, having nominal gas flow rate for helium referred to vacuum equal to 1.2×10^{-6} mbar L/s and 1.2×10^{-5} mbar L/s respectively at the inlet pressure of 1 bar.

2.2. Metal Leaks

Three different materials were used to realize the metal leak artefacts: stainless steel, copper and aluminium. These materials are easily available and compatible with all vacuum ranges and regular holes can be "drilled" by laser technology. Fig. 2 shows the different leak artefacts prepared at INRIM. For the stainless steel type, one side of a double knife flanges was reduced to 0.8 mm by electro-erosion, then it was polished. For the copper and aluminium type, disks having the same dimension of standard CF16 flange gasket were used. The central area on one side of each disk was lowered to 0.4 mm by mechanical process. Into this area small holes having nominal diameters from 20 µm to 8 µm were drilled by laser technology. Laser micro-drilling is the process of removing material from a solid surface by irradiating it with a laser beam focused into a very small spot able to melt and vaporize the material. Laser ablation strongly depends on laser characteristics and target properties. The laser pulse duration and irradiance are the most important factors for defining ablation conditions.

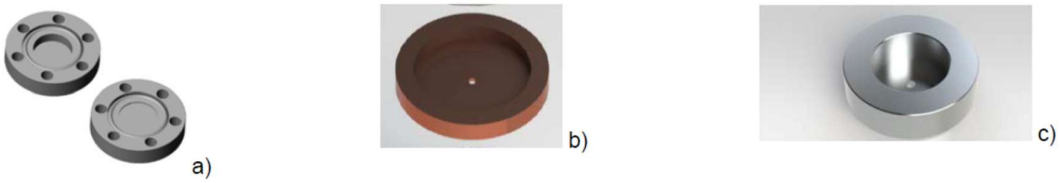

Fig.2 Metal capillaries a) stainless steel double knife CF 16 flanges; b) copper disk; c) aluminium disk

Reducing pulse duration has the effect of reducing thermal penetration depth and increasing irradiance, so the removal process is dominated by vaporization rather than melting and accuracy increases. Another important parameter in laser ablation process is the laser wavelength. Shorter wavelengths offer the best laser-material coupling, particularly with dielectrics, but also with metals (reflectivity of most metals decreases at shorter wavelengths). RTM SpA, realized the holes by a Diode-Pumped Solid State laser having: short wavelength (532 nm), focused beam diameter of 15 µm, pulse energy of the order of 1 mJ, short pulse duration (nanosecond regime), and a radiation flux density in the processing zone of about 1 GW/cm^2.

As example, the Fig. 3 shows the hole obtained on a SS double knife flange as received by the manufacturer; on the side where the laser beam pierces a deposition of material has been observed. At INRIM nanofacilities a Focused Ion Beam (FIB) instrument having micromachining capabilities at the nanometer–micrometer scale was used to remove the material around the hole.

The same procedure was applied to all the samples and only those having the more regular holes were chosen and used to perform the measurements by NMI partners in the project.

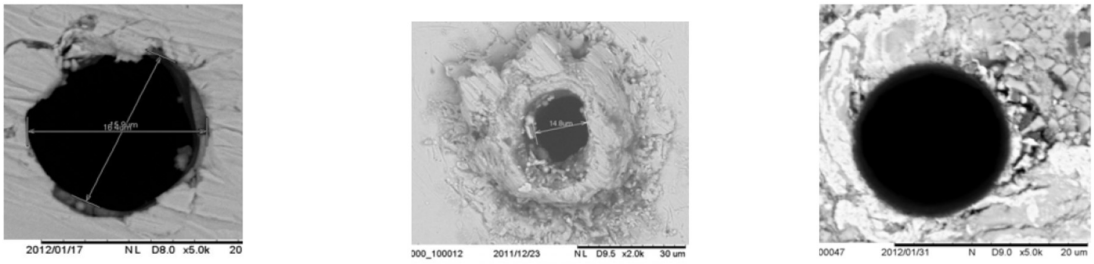

Fig. 3 SEM pictures of the hole a) Laser beam outlet; b) Laser beam inlet ; c) Hole after FIB cleaning

2.3 Geometrical measurement of the leak artifacts

Thickness of the leaks artefacts

The thickness of the plate has been measured with a 1D linear comparator (Moore M3) equipped with a laser interferometer. A mechanical probe is used to determine the starting and the ending points of the interferometric displacement measurement, whereas the mechanical probe diameter is determined by using a calibrated gauge block. Measurements were carried out in different symmetrical positions and repeated two times in the lowered area of the flanges/disks.

Metal micro-holes diameters

A 2-D grating was used as reference to measure the hole diameter of the leaks. A 2-D grating is a flat surface on which equally spaced straight and parallel grooves of equal profile and a second series of similar grooves orthogonal to the first are engraved. Therefore the surface is transformed in a rectangular matrix structure. Each cross section of the grating is represented as a rectangular periodic function in space with period p called "pitch" of the grating.

The measurand is the mean distance between the grooves in the surface area illuminated by the laser beam of the INRIM diffractometer. The grating pitch p is determined by measuring the angle of autocollimation related to a laser beam having a specific wavelength. The traceability to SI is obtained through the INRIM standards of angle and length (He-Ne laser 127 (I2)). The pitch p of the grating used in our measurements is p = 462.92 nm with standard uncertainty of 0.03 nm.

As first step, a SEM image of the grating using a magnification x5k, was taken. Starting from the grating calibration a length of 26.17 nm ± 0.26 nm was associated at each pixel. The calibration uncertainty of the pitch is negligible compared to the uncertainty of pitch definition.

As second step, the hole pictures with a magnification x5k were taken and by means of an image processing software the coordinates of the profile border were identified and recorded (Fig. 4). From the recorded coordinates the diameter for each hole was calculated.

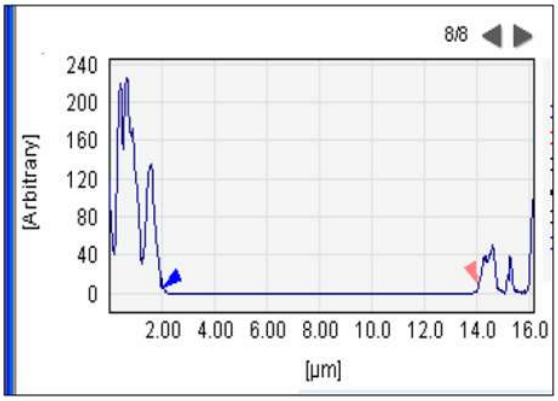

Fig. 4 example of a profile image: the marks shown the measurement points

The standard deviation of the diameter measurements obtained in the different positions, for each side of the flange/disk, may be considered as deviation from the ideal circle. A difference between the hole diameters of the two sides of flange/disk is pointed out from measurements. The main components of the standard uncertainty *u* are the standard deviation of the mean of measurements and the uncertainty due to circle shape definition.

The following table presents the dimensions of the different artefacts, diameters of each side and length of leak elements. Uncertainties associated to these measurements are reported, and are typically lower than 3 % except for diameters below 10 µm for which relative uncertainties are less than 4 %. The glass leak is not mentioned in the table 1, as it was not possible to measured the restriction diameter by SEM, to quantify its dimensions.

Leak artefact	Diameter ($1 \cdot 10^{-6}$ m)		u(d) ($1 \cdot 10^{-6}$ m)		Length (1.10^{-3} m)	u(l) (1.10^{-3} m)
	Side1	Side2	Side1	Side2		
SS leak B1	14.80	15.95	0.30	0.27	0.7450	0.0028
SS leak B2	16.54	5.63	0.30	0.27	0.7702	0.0028
SS leak C1	19.48	17.70	0.31	0.33	0.8088	0.0012
Copper leak D1	11.40	9.86	0.31	0.37	0.3523	0.0024
Aluminium leak E1	11.81	6.12	0.34	0.26	0.3633	0.0025
Aluminium leak E2	12.28	6.94	0.29	0.27	0.3857	0.0033
Glass fiber	43.20		0.93		0.720	0.001

Table 1 Measured diameters and thickness for several leaks

To make the artefacts available for measurements and robust (i.e. easy mounting on the various NMIs primary flowmeters), each hole was encased in a suitable fitting with the upstream side defined. In

case of conical shapes, the larger diameter was chosen to be directed to the higher pressure. Tightness of the seal was lower than 10^{-10} mbar L/s.

3. NMI's primary systems

Four NMIs, CMI, INRIM, LNE, PTB, and a calibration service laboratory, THM, participated in the characterization of the leaks both with expansion to vacuum and to atmosphere by using their own primary flowmeters which are based on different methods: constant pressure flowmeter, constant volume flowmeter, photoacoustic method and laminar flow element method.

Constant pressure and variable-volume method

The method allows flows determination through time derivation of the ideal gas equation $p_M V_M = n R T$, that relates, through the ideal gas constant R, the number n of gas moles, contained in a measurement volume V_M (at a temperature T), to the volume V_M itself and to the pressure p_M in it. In Fig. 5 a general scheme of a primary flowmeter is shown: the volumes V_R and V_M are the reference and measurement volumes, respectively, while V is the inlet or outlet volume of the flow (for gas flows referred to vacuum or atmospheric pressure, respectively). In the initial configuration of the system, V_R and V_M are connected each other, at the same pressure $p_M = p_0$; V is isolated and maintained at the pressure p (with $p \neq p_M$). At the instant t_0, acting in quick succession, V_M is separated from V_R by closing valve v_A, and connected to V, by opening valve v_B. The pressure difference at the ends of the leak generates a gas flow from V_M to V (if $p_M > p$), or vice versa. The two possible types of flow that are currently measured can be summarized as follows:

- flows referred to vacuum ($p_M > p$): p_M (that is the upstream pressure of the leak) can be varied from about 70 Pa up to a maximum of about 10^5 Pa, while the downstream pressure p has a value negligible to the upstream pressure
- flows referred to atmospheric pressure ($p_M < p$): p_M (that is the downstream pressure of the leak) is about 100 kPa, while p (that is the upstream pressure) can be varied from about 1.2×10^5 Pa up to about 2×10^5 Pa.

In practice, the molar flow q_m, coming out of the volume V_M through the standard leak or coming in V_M, according to the type of flow measurement, if referred to vacuum or atmospheric pressure, respectively, is measured varying the volume V_M itself in such a way to maintain its internal pressure at a constant value p_0. Therefore, under the hypothesis that the temperature T is constant, the following relation can be directly obtained time-deriving the ideal gas law:

$$q_m = \frac{dn}{dt} = \frac{p_0}{RT} \cdot \frac{\Delta V_M}{\Delta t} = \frac{q_{pV,p}}{RT} \qquad (1)$$

where $q_{pV,p}$ is the throughput rate measured by constant pressure – variable volume flowmeter

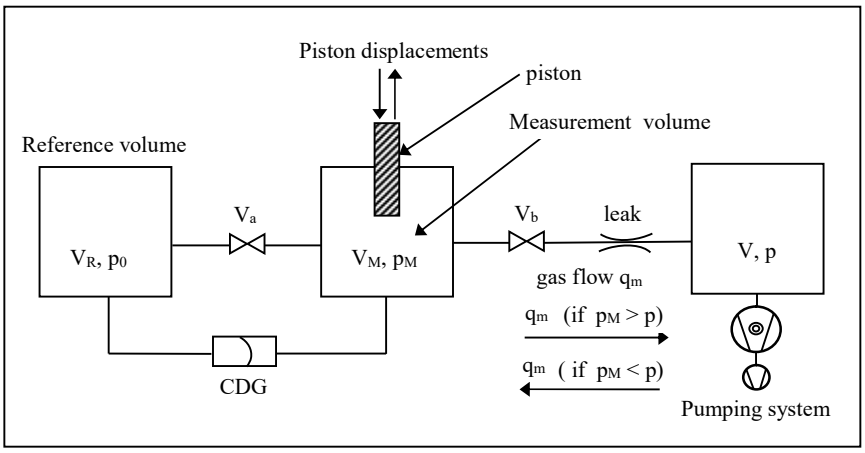

Fig.5 Scheme of the flowmeters based on constant pressure and variable-volume method

The pressure difference (p_M - p_0), measured with the capacitance diaphragm gauge (CDG), is used to control the piston displacement (up or down depending on the flow direction) in order to maintain constant the pressure in the measurement volume.

Constant volume and variable pressure method (pressure rise method)

In case of constant volume – variable pressure method a formula similar to (1) is used to measure the molar gas flow rate q_m, which is determined measuring the variation of pressure as function of time inside the constant volume V_M; under the hypothesis that the temperature T is constant, the equation (2) can be directly obtained time-deriving the ideal gas law:

$$q_m = \frac{V_M}{RT} \cdot \frac{\Delta p_M}{\Delta t} = \frac{q_{pV,V}}{RT} \qquad (2)$$

In which $q_{pV,V}$ is the throughput rate measured by constant volume method and the volume V_M was previously determined by a different experiment.

As example, a relatively easy method to measure the volume V_M consists in determining a throughput rate by constant pressure- variable volume method; then the same throughput is measured by pressure rise method and comparing the two results it is possible to calculate the volume V_M.

Photoacustic method

As the refrigerant gases absorb at wave lengths in the infrared range, infrared detection is particularly suitable to measure the concentration of a refrigerant gas. The method developed at LNE consists in measuring the accumulation of the gas emitted by the refrigerant leak in an enclosed “accumulation

volume" under atmospheric pressure, as shown in Fig. 6. The rise of the refrigerant gas concentration is then measured by an infrared photoacoustic spectrometer.

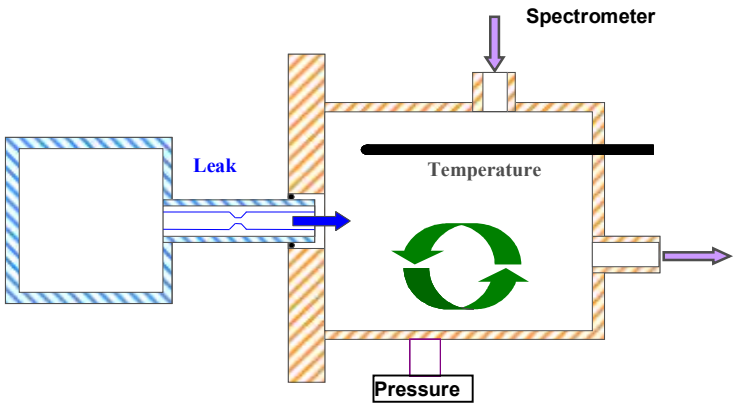

Fig. 6 Scheme of the system to measure gas flows supplied through the leak in calibration

The flow rate can be calculated using the equation:

$$q_m = \frac{MV}{R} \cdot \frac{\partial}{\partial t}\left(\frac{p \cdot C}{T}\right) \quad (3)$$

Where M is the molar mass of the gas, V is a volume calibrated by a static expansion method, R is the ideal gas constant, p and T are the pressure and temperature inside the volume V, C is the gas concentration measured by the infrared photo-acoustic spectrometer.

Laminar flow element method

The laminar flow element method is shown in Fig.7. The laminar flow element measures the mass flow of the gases indirectly by measuring the temperature and the inlet and outlet pressures. The pressure difference across a pipe is directly proportional to the flow rate. Laminar flow conditions are present in a gas when the Reynolds number of the gas is below the critical figure. The viscosity of the fluid is compensated.

The used laminar flow elements are constructed as a cylindrical interstice between inner and outer cylinders to achieve the required flow rate. The laminar flow elements are utilized as the secondary standards with the direct traceability to the primary gravimetric flow standard (GFS). The GFS principle is based on the measurement of the weight loss of the gas in the bottle. This makes it possible to ensure the traceability for different gases.

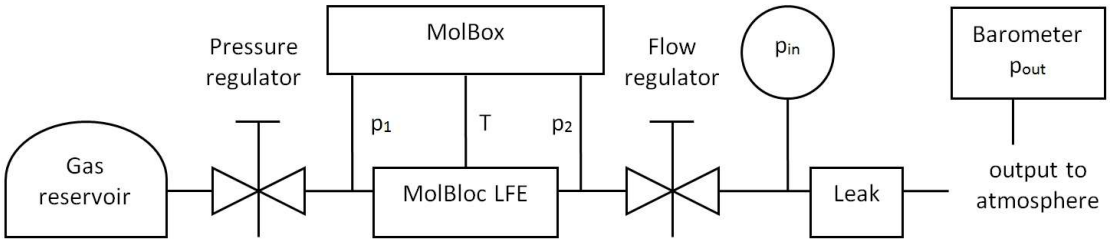

Fig.7 Schematic of laminar flow element method. The gas from the reservoir is passing through MolBloc laminar flow element and through the leak to the atmosphere. The leak inlet and outlet pressures are measured using two absolute pressure gauges.

In the table 2 the methods and related uncertainty of the participating national metrology institutes are listed.

NMI	Method	Gas flow range (mol s^{-1})	Uncertainty ($k = 2$)
CMI	Constant pressure method (vacuum)	$4x10^{-12} \div 3x10^{-5}$	$8x10^{-14}$mol s^{-1} + 1.2 $x10^{-2}$ x q
CMI	Laminar flow elements (atmosphere)	$7x10^{-8} \div 2x10^{-2}$	0.3 %
INRIM	Constant pressure method (atmosphere)	$4x10^{-10} \div 2x10^{-7}$	4.6% ÷ 0.4%
INRIM	Constant pressure method (vacuum)	$4x10^{-10} \div 2x10^{-7}$	2.1% ÷ 0.3%
LNE	Constant pressure method (atmosphere)	$4x10^{-10} \div 8x10^{-7}$	$9x10^{-11}$ mol s^{-1} + 0.1x 10^{-2} x q
LNE	Photo acoustic method (R134-a atmosphere)	$3x10^{-10} \div 2x10^{-8}$	2% to 5%
LNE	Constant volume method (vacuum)	$8x10^{-11} \div 2x10^{-6}$	1% to 4%
PTB	Constant pressure method (vacuum)	$1x10^{-14} \div 4x10^{-9}$	5.0% to 1.2%
PTB	Constant pressure method (atmosphere)	< $7x10^{-9}$ mol/s	1% to 2%
PTB	Pressure rise method (atmosphere)	> $3x10^{-9}$ mol/s	10%

Table 2 Uncertainly of NMIs facilities

4. Measurements results

The measurand is the gas flow generated through the considered standard leak when a well-known pressure drop $\Delta p = p_u - p_d$ is established between inlet and outlet (p_u and p_d indicate respectively the upstream/inlet and the downstream/outlet pressures). The molar flow rate q_m (SI unit: mol s^{-1}) is used as it gives the amount of gas which flows through the leak per time unit. The leak rate in this unit is independent of the gas temperature.

In the following table 3 the experimental conditions of the leak artefacts calibrations are shown.

NMI	Leak	Gases	Pressure difference Δp applied
CMI	SS leak C1	He, N2, H2, Ar, SF6, R134a, CO2, 1234yf	50 Pa ÷ 100 kPa (vacuum) 2 kPa ÷400 kPa (atmosphere)
CMI	Glass leak H1	He, N2, H2, Ar, SF6	50 Pa ÷ 100 kPa (vacuum) 2 kPa ÷400 kPa (atmosphere)
INRIM	Cupper leak D1	He, N2, N2/H2 (95/5), Ar, R134a, CO2, R12	50 Pa ÷ 100 kPa (vacuum) 2 kPa ÷ 150 kPa (atmosphere)
INRIM	Glass fiber	He, N2, Ar, R134a	2.5 kPa ÷100 kPa (atmosphere)
LNE	Aluminium leak E2	He, N2, N2/H2 (95/5), Ar, SF6, R134a, CO2, R12	50 Pa ÷ 150 kPa (vacuum) 2 kPa ÷400 kPa (atmosphere)
LNE	SS leak B1	He, N2, N2/H2 (95/5), Ar, SF6, R134a, CO2	50 Pa ÷ 150 kPa (vacuum) 2 kPa ÷100 kPa (atmosphere)
PTB	Aluminium leak E1	He, N2, H2, Ar, SF6, R134a, CO2	50 Pa ÷ 100 kPa (vacuum) 2 kPa ÷400 kPa (atmosphere)
THM	SS leak B2	He	150 kPa ÷ 4 MPa (vacuum)

Table 3 Experimental conditions of calibrations

It was decided to use different working fluids having the molar mass from 2 g/mol (hydrogen) to 146 g/mol (SF6) in a wide range of Δp from 50 Pa to 400 kPa. Consequently the flow-regime from free molecular to hydrodynamic in the ducts can be featured and an extensive comparisons between experimental molar flow rates and the predictions with different numerical models can be carried out.
The experimental data are comprehensively collected and available online as background dataset. To give to the readers an idea of the data trend, the conductance C was calculated by using the equation:

$$qRT = C\Delta p \tag{4}$$

where Δp is the pressure difference in Pa.
The conductance depends on the gas species, but it is possible to overcome it by calculating the normalized conductance using the following equation:

$$C_n = C\sqrt{M_g} \tag{5}$$

where M_g is the molar mass of the gas.
As examples, in the figures 8 to 15, the normalized conductance is plotted versus the inverse 1/λ of the mean free path:

$$\lambda = 116.4\frac{\eta}{p_a}\cdot\sqrt{\frac{T}{M_g}} \tag{6}$$

where p_a is the mean pressure inside the leak, T, M_g and η are respectively the absolute temperature, the molar mass and the dynamic viscosity of the gas .

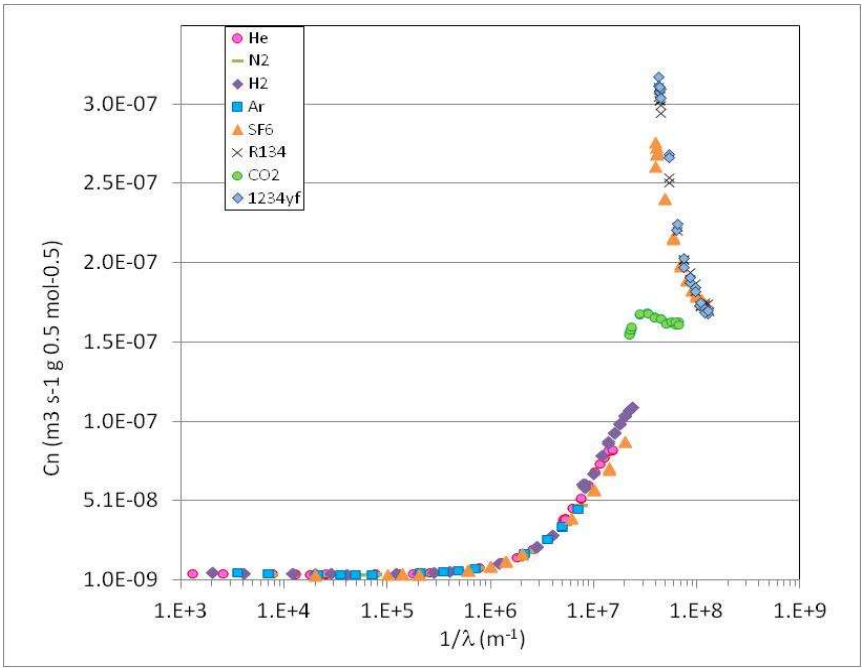

Fig. 8 Normalized conductance versus inverse mean path for leak C1

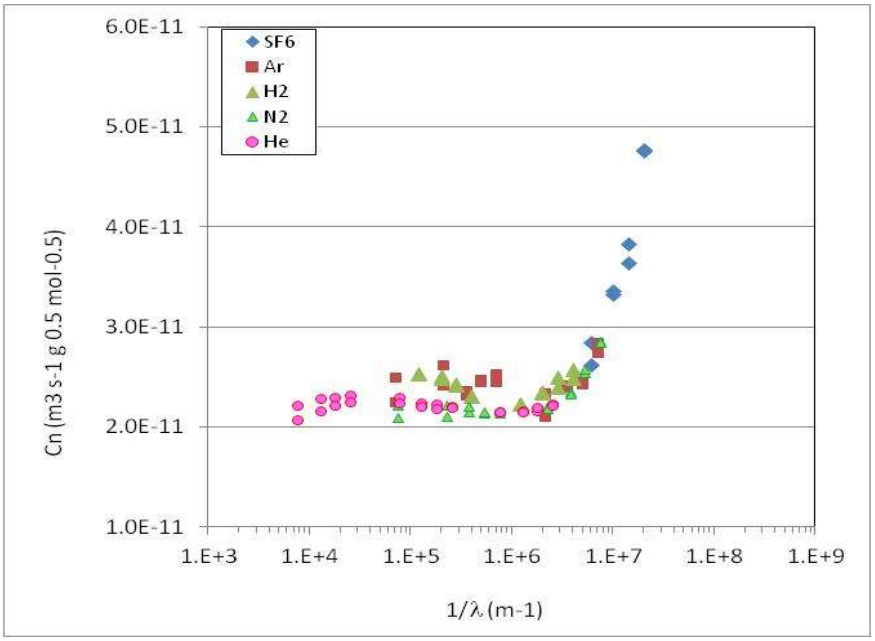

Fig. 9 Normalized conductance versus inverse mean path for leak H1

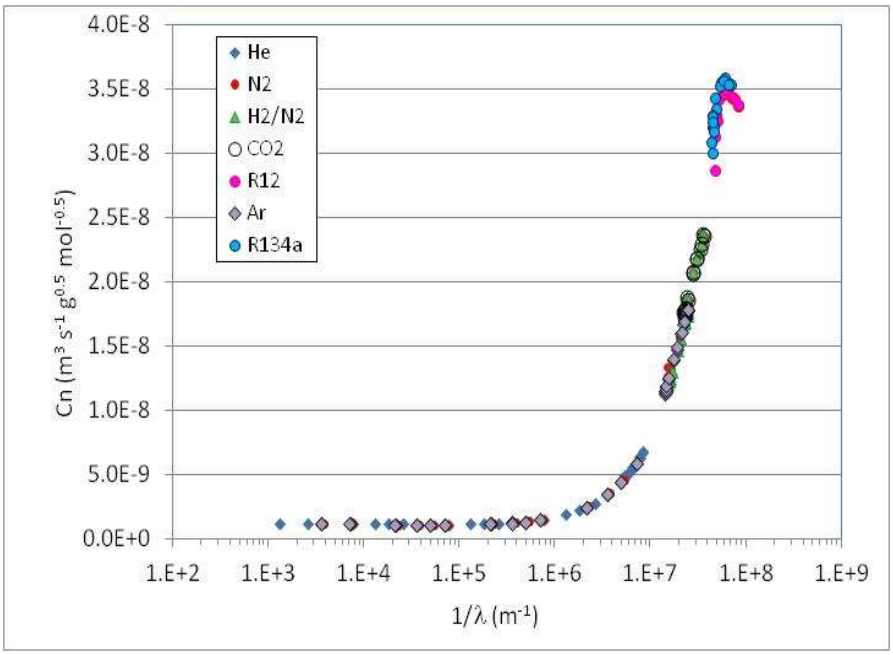

Fig. 10 Normalized conductance versus inverse mean path for leak D1

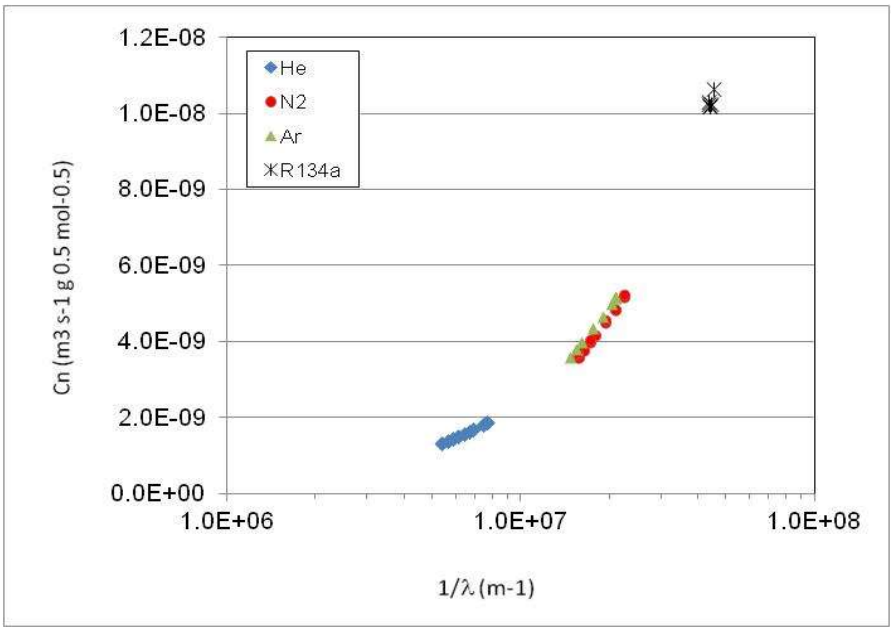

Fig.11 Normalized conductance versus inverse mean path for glass fiber leak

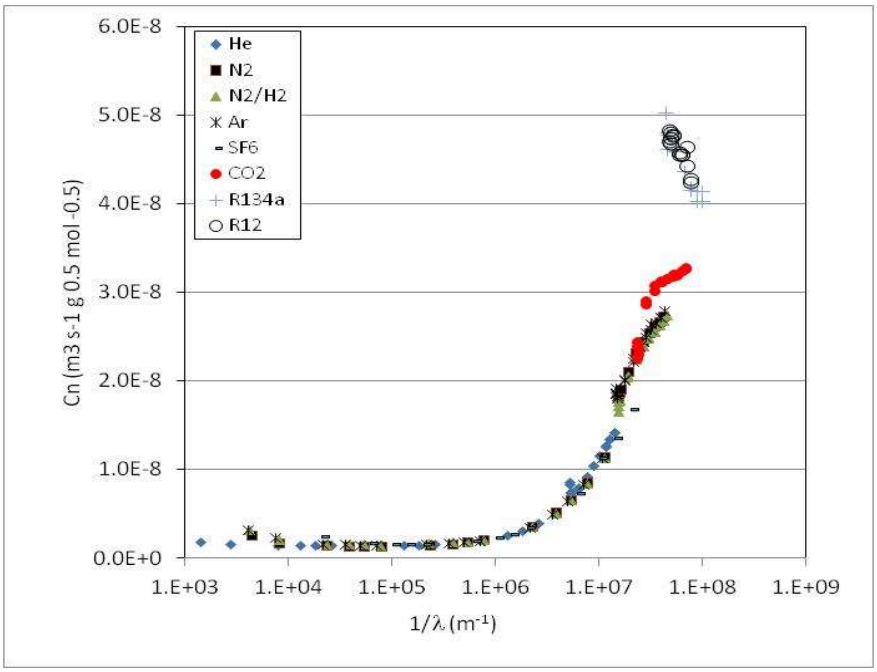

Fig. 12 Normalized conductance versus inverse mean path for leak E2

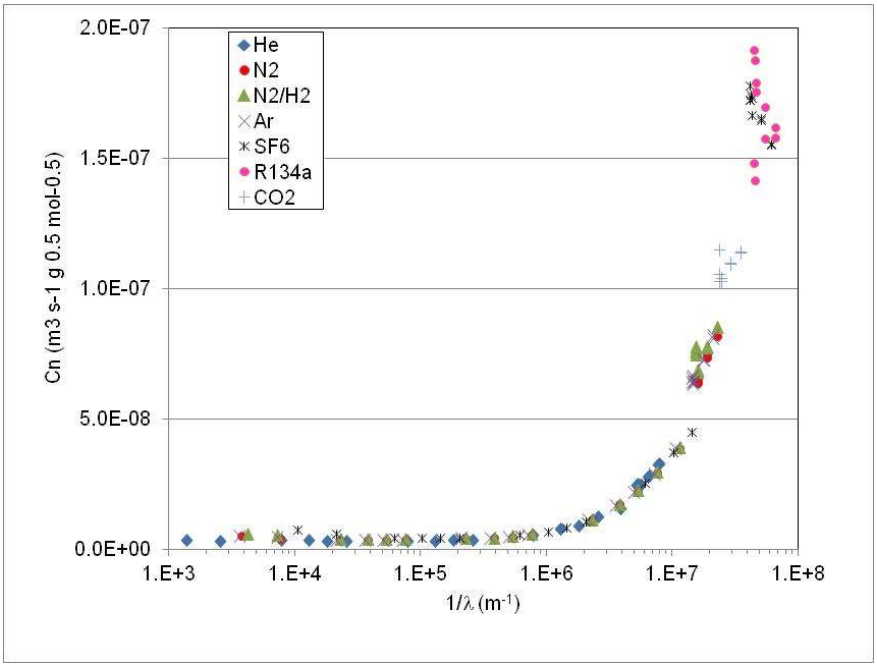

Fig. 13 Normalized conductance versus inverse mean path for leak B1

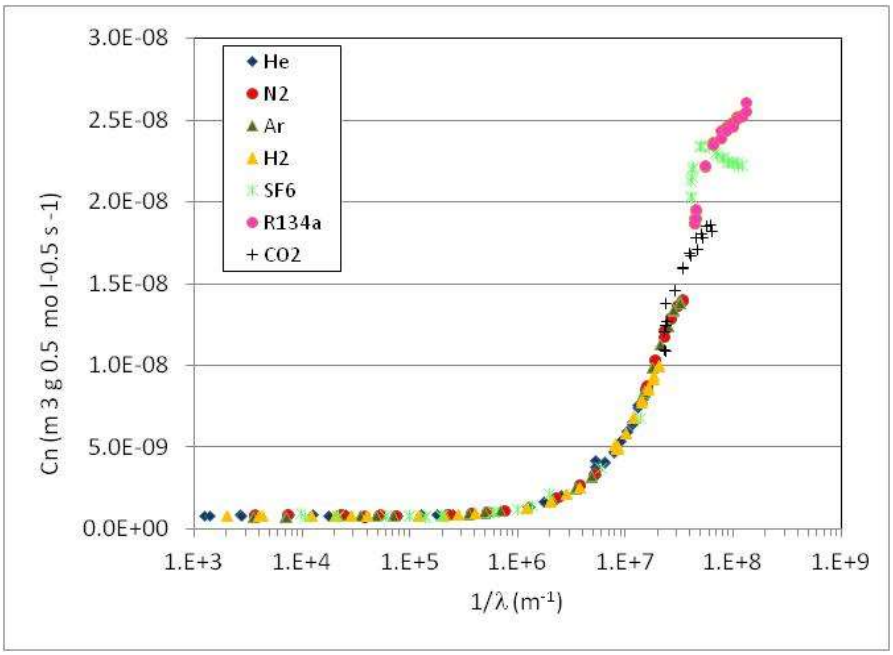

Fig. 14 Normalized conductance versus inverse mean path for leak E1

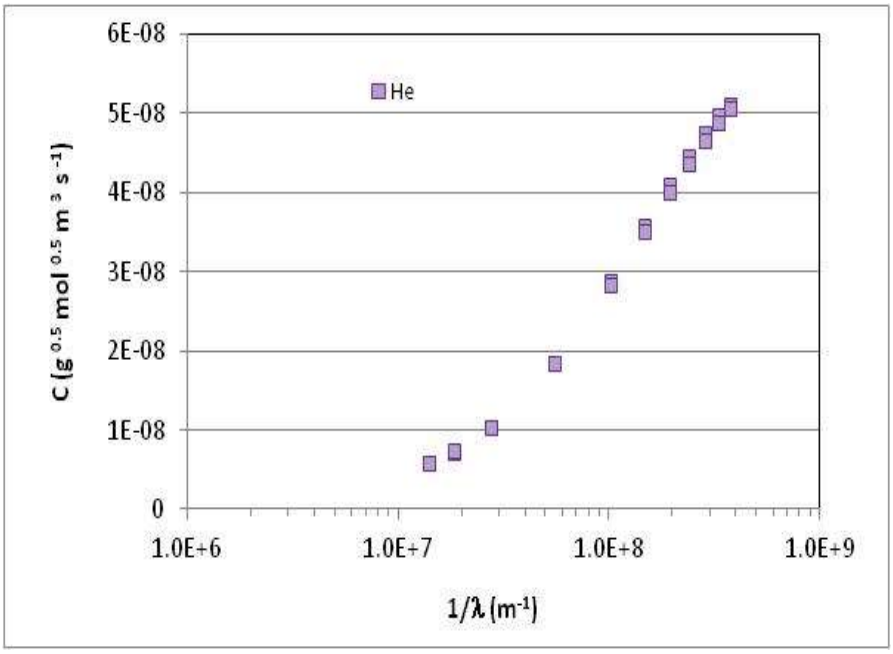

Fig. 15 Normalized conductance versus inverse mean path for leak B2

From figures, the existence of the regimes from molecular to hydrodynamics is pointed out. In some case the data had to be cleaned from the anomalous data probably due to the lack of performance of the primary systems.

5. Conclusion

Several reference leaks were realized in the framework of the European project JRP IND12, Vacuum metrology for production environments, to improve the knowledge of gas flow through micro-channels, in particular in terms of predictability for different gas species.

The leaks were made with different materials and geometry and calibrated with reference to vacuum and to atmospheric pressure. More than 800 data were collected by four National Metrological Institutes (CMI, INRIM, LNE, PTB) and one calibration service laboratory (THM), considering different gas species and different inlet pressure.

The measurement were carried out in a wide gas flow rate range between $1x10^{-8}$ mol s^{-1} and $7x10^{-6}$ mol s^{-1} to cover different gas flow regimes from the molecular to hydrodynamic regime.

The experimental data are comprehensively collected and available online as background dataset, in order to make available to scientific community a large amount of data, which could be used to improve the knowledge of the mathematical models describing the gas flow regimes inside the leaks.

Acknowledgement

This work was supported by EMRP IND12 project. The EMRP is co-financed by EMRP participants within EURAMET and the European Union.

The authors wish to thank S. Pasqualin (INRIM) for the fruitful help during the realization of the leaks.

References

[1] A. Calcatelli, M. Bergoglio and D. Mari, Leak detection, calibrations and reference flows: practical example, Vacuum 81,11-12 (2007) 1538-1544

[2] M. Bergoglio, G. Brondino, A. Calcatelli, G. Raiteri, G. Rumiano, Mathematical model applied to the experimental calibration results of a capillary standard leak, Flow Measurement and Instrumentation 17 (2006) 129–138

[3] M. Bergoglio, G. Raiteri, G. Rumiano, W. Jitschin, Intercomparison of gas flow-rate measurements at IMGC-CNR, Italy, and UASG, Germany, in the range 10_8–10_3 Pam3/s, Vacuum 80 (2006) 561-567

[4] M. Bergoglio, D. Mari, INRIM primary standard for micro gas flow measurements with reference to atmospheric pressure, Measurement 45 (2012), 2459-2463

[5] M. Bergoglio, D. Mari, INRIM continuous expansion system as high vacuum primary standard for gas pressure measurements below $9 \cdot 10^{-2}$ Pa, Vacuum 84, 1 (2009) 270-273

[6] K. Jousten, , U. Becker, A primary standard for the calibration of sniffer test leak devices, Metrologia 46 (2009), 560-568

[7] K Jousten, H Menzer, R Niepraschk, A new fully automated gas flowmeter at the PTB for flow rates between 10^{-13} mol/s and 10^{-6} mol/s, Metrologia 39 (2002), 519–529

[8] T. Gronych, L. Peksa, P. Řepa, J Wild, J Tesař, D. Pražák, Z. Krajíček, M. Vičar, The use of diaphragm bellows to construct a constant pressure gas flowmeter for the flow rate range 10^{-7} Pa m^3 s^{-1} to 10^{-1} Pa m^3 s^{-1}, Metrologia 45 (2008), 46–52

[9] F. Boineau, Characterization of the LNE constant pressure flowmeter for the leak flow rates measurements with reference to vacuum and atmospheric pressure, PTB mitteillungen 3/2011 – Proceedings 5th CCM international conference (2011), 313-316